



Contribution to Special Issue: 'Towards a Broader Perspective on Ocean Acidification Research' Original Article

Micro-CT analysis of the Caribbean octocoral *Eunicea flexuosa* subjected to elevated $p\text{CO}_2$

I. C. Enochs^{1,2*}, D. P. Manzello², H. H. Wirshing³, R. Carlton^{1,2}, and J. Serafy⁴

¹Cooperative Institute for Marine and Atmospheric Studies, Rosenstiel School of Marine and Atmospheric Science, University of Miami, 4600 Rickenbacker Cswy, Miami, FL 33149, USA

²Atlantic Oceanographic and Meteorological Laboratory, NOAA, 4301 Rickenbacker Cswy, Miami, FL 33149, USA

³Smithsonian Institution, National Museum of Natural History, PO Box 37012, MRC 163, Washington, DC 20013-7012, USA

⁴Southeast Fisheries Science Center, NOAA, 75 Virginia Beach Dr, Miami, FL 33149, USA

*Corresponding author: tel: +1 305 361 4399; fax: +1 305 361 4447; e-mail: ienochs@rsmas.miami.edu

Enochs, I. C., Manzello, D. P., Wirshing, H. H., Carlton, R., and Serafy, J. Micro-CT analysis of the Caribbean octocoral *Eunicea flexuosa* subjected to elevated $p\text{CO}_2$. – ICES Journal of Marine Science, 73: 910–919.

Received 17 March 2015; revised 8 July 2015; accepted 19 August 2015; advance access publication 12 September 2015.

Rising anthropogenic carbon dioxide has resulted in a drop in ocean pH, a phenomenon known as ocean acidification (OA). These acidified waters have many ramifications for diverse marine biota, especially those species which precipitate calcium carbonate skeletons. The permanence of coral reef ecosystems is therefore closely related to OA stress as habitat-forming corals will exhibit reduced calcification and growth. Relatively little is known concerning the fate of other constituent taxa which may either suffer concomitant declines or be competitively favoured in acidified waters. Here, we experimentally (49 d) test the effects of next century predictions for OA ($\text{pH} = 7.75$, $p\text{CO}_2 = 1081 \mu\text{atm}$) vs. near-present-day conditions ($\text{pH} = 8.01$, $p\text{CO}_2 = 498 \mu\text{atm}$) on the common Caribbean octocoral *Eunicea flexuosa*. We measure linear extension of this octocoral and use a novel technique, high-resolution micro-computed tomography, to measure potential differences in the morphology of calcified internal skeletal structures (sclerites) in a 2 mm apical section of each branch. Despite the use of highly accurate procedures, we found no significant differences between treatments in either the growth of *E. flexuosa* branches or the structure of their sclerites. Our results suggest a degree of resilience to OA stress and provide evidence that this octocoral species may persist on Caribbean coral reefs, despite global change.

Keywords: calcification, micro-CT, ocean acidification, octocoral, sclerite.

Introduction

Anthropogenic carbon dioxide has resulted in a 0.11°C increase in sea surface temperature (SST) since the 1970s, and current estimates predict a further $0.6\text{--}2.0^\circ\text{C}$ rise by the end of the century (Collins *et al.*, 2013; Rhein *et al.*, 2013). Rising atmospheric carbon dioxide has been accompanied by an increase in the partial pressure of CO_2 ($p\text{CO}_2$) in ocean water. This phenomenon, known as ocean acidification (OA), is responsible for a decline of 0.1 pH units since the preindustrial era and an estimated drop of another 0.14–0.35 pH units by the end of the century (IPCC, 2007; Rhein *et al.*, 2013).

The resulting warmer and more-acidic seas associated with global change will have widespread impacts on marine ecosystems, perhaps most notably coral reefs, which are hotspots of biodiversity

(Reaka-Kudla, 1997; Kleypas *et al.*, 1999; Hoegh-Guldberg *et al.*, 2007). Reef-building or hermatypic scleractinian corals within the cnidarian subclass Hexacorallia are currently distributed close to their maximum thermal tolerance, making them especially sensitive to rising temperatures associated with global change. Protracted periods above this threshold can result in expulsion of symbiotic zooxanthellae (dinoflagellates in the genus *Symbiodinium*), leading to coral mortality and reef degradation if stress is not quickly ameliorated (Baker *et al.*, 2008). OA will also negatively influence reef health via many mechanisms directly impacting the corals themselves, including reduced calcification (Langdon and Atkinson, 2005) and recruitment (Albright *et al.*, 2010). OA may also affect many other taxa (Kuffner *et al.*, 2007; Johnson *et al.*, 2012; Bignami *et al.*, 2013; Enochs *et al.*, 2015), disrupt competitive

hierarchies (Diaz-Pulido *et al.*, 2011; Kroeker *et al.*, 2012), and favour communities dominated by taxa other than hermatypic corals. For some species, however, short-term experimental studies and real-world systems have revealed no significant adverse effects of OA and low carbonate saturation states (Ω), providing nuance to the concept of OA as a universal stressor (Kroeker *et al.*, 2010; Cryonak *et al.*, 2016; Jokiel, 2016).

Regardless, the influence of OA and other anthropogenic stressors is already apparent in the Caribbean. In the last 30 years, average coral cover on reefs in this region has dropped by roughly 80% (Gardner *et al.*, 2003). The resulting lower calcification and high rates of erosion have contributed to a drop in structural complexity (Alvarez-Filip *et al.*, 2009) that likely has influenced associated fish and invertebrate populations (Graham and Nash, 2013). Currently, it is believed that as reefs degrade in structural complexity and coral cover, they will be replaced with larger proportions of macroalgae, potentially shifting into a less desirable alternative stable state (Hoegh-Guldberg *et al.*, 2007). Evidence from a volcanic CO₂ vent off Japan, however, revealed healthy octocoral communities in low pH water, suggesting a shift from hexacorals to octacorals under OA conditions (Inoue *et al.*, 2013).

Relative to hermatypic hexacorals, octacorals are poorly studied. This is unfortunate considering their high abundances (Lasker and Coffroth, 1983; Yoshioka and Yoshioka, 1989; Ruzicka *et al.*, 2013) and diversity (Alcolado *et al.*, 2003; Guzmán, 2003) among coral reef and hard bottom habitats throughout the Florida Keys and Caribbean. In these and other environments, octacorals fulfil a number of important ecological roles, including trophic and habitat functions, by consolidating and forming carbonate substrates as well as providing shelter to invertebrates and fish (Goh *et al.*, 1999; Glynn and Enochs, 2011; Jeng *et al.*, 2011).

Current data on the effects of OA on octacorals are mixed. Bramanti *et al.* (2013) found that the non-reef-dwelling red coral *Corallium rubrum*, collected from deep temperate waters in the Mediterranean, exhibited significantly reduced skeletal growth, abnormally shaped sclerites, and increased total organic matter at a pH of 7.81. In contrast, Gabay *et al.* (2013) found no significant differences in three species of octocoral from Eilat, even after prolonged exposure (up to 5 months) under pH conditions as low as 7.6 and 7.3. At these extremely reduced pHs, however, sclerites free of living tissues were found to degrade, but those that were maintained inside of living specimens were intact, suggesting a degree of protection to OA stress conferred by the living coral (Gabay *et al.*, 2014). Inoue *et al.* (2013), working with *Sarcophyton elegans* from reefs off Japan, found that elevated $p\text{CO}_2$ enhanced photosynthesis and significantly increased night-time decalcification, but did not significantly impact daytime calcification. Finally, the only study to date on the influence of OA on a Caribbean octocoral was conducted by Gómez *et al.* (2014). Working with *Eunicea fusca*, they found that a reduction in pH consistent with IPCC projections for the end of the century (7.8) resulted in a slight increase in growth and calcification. However, over the full spectrum of OA treatments that Gómez *et al.* (2014) applied (down to 7.1), there was a significant negative relationship between OA and all measured growth metrics, including buoyant weight, linear extension, and per cent incorporation of calcein stain into sclerites.

Perhaps, the lack of a consistency in the response of previously studied octacorals to OA is due to the great diversity of both colony and skeletal morphologies present among these taxa. Further work is therefore needed to more clearly understand the response of these taxa to OA. To this end, we experimentally tested the effects

of elevated $p\text{CO}_2$ on the growth of sclerites and branch tips of the Caribbean octocoral *Eunicea flexuosa*. We employed high-resolution micro-computed tomography (micro-CT), for *in situ* quantification of growth and skeletal metrics. While micro-CT technology has previously been applied to octacorals in a methods paper to identify and map internal canal networks (Morales Pinzón *et al.*, 2014), our study is the first to quantify calcified structures within an octocoral and use these data to statistically compare treatment groups.

Methods

Experimental manipulations

Four colonies of *E. flexuosa* were collected from ~7 m depth at Cheeca Rocks, Florida Keys. Colonies were transported to laboratory facilities at the University of Miami (Key Biscayne, FL, USA) where they were fragmented into seven to eight individual branches (~10 cm length) and affixed to labelled PVC tiles using underwater epoxy (All-Fix). The resulting replicates were divided among eight experimental tanks (15 in high CO₂, 14 in low CO₂) for 49 d. An additional apical branch tip from each of the parent colonies was removed at the time of collection and immediately preserved in EtOH for subsequent scanning of initial branch characteristics.

Each of the eight independent experimental systems consisted of two connected ~75-l tanks, the top of which contained the *E. flexuosa* replicates and a circulation pump (Figure 1). Temperature and carbonate chemistry were manipulated in the lower of the two tanks. Temperature was maintained at 25°C through the use of a chilled water bath and aquarium heaters. Treatment gas was introduced into each tank using a venturi pump at a constant flow rate regulated with a valved variable area flowmeter (Cole Parmer). A target OA treatment level of 1000 μatm was set based on IPCC predictions for roughly 100 years from now, assuming the continued reliance on fossil fuel-based energy technologies (IPCC, 2007, model A1F1). The concentration of the enriched CO₂ treatment gas was precisely regulated using mass flow controllers (Sierra Mass-Trak 810C), compressed air, and pure CO₂. Fresh seawater was dripped into each system at a rate so that the entire volume of the system was refreshed multiple times per day. The experiment was performed in a blacked-out room with artificial light (two 216 W T5 fixtures) illuminating on a 12 h cycle.

The temperature, salinity, and pH of each tank were measured three times per week using a hand-held YSI Professional Plus multiprobe unit. Seawater $x\text{CO}_2$ was measured five times per week from 11 February to 7 March using a non-dispersive infrared CO₂ gas analyser (LI-COR, LI-810), connected to air-gas equilibrator (General Oceanics). Discrete water samples were collected from each tank one to two times weekly for analysis of dissolved inorganic carbon (DIC) and total alkalinity (TA). Both parameters were measured using ApolloSciTech instruments (AS-C3 and AS-ALK2, DIC and TA, respectively). Temperature, salinity, DIC, and TA were used to calculate $p\text{CO}_2$ using the CO2SYS software package (Lewis and Wallace, 1998) and the dissociation constants of Mehrbach *et al.* (1973), as refit by Dickson and Millero (1987) and Dickson (1990) for boric acid.

To minimize tank effects, every 2 weeks, replicates of *E. flexuosa* were randomly reassigned to different tanks within the same treatment (high vs. low CO₂). The height of each *E. flexuosa* branch was measured at the beginning and end of the experiment using Vernier calipers to determine linear extension. The tips of each branch were removed following the experiment, preserved in 70% EtOH, and reserved for analysis using micro-CT.

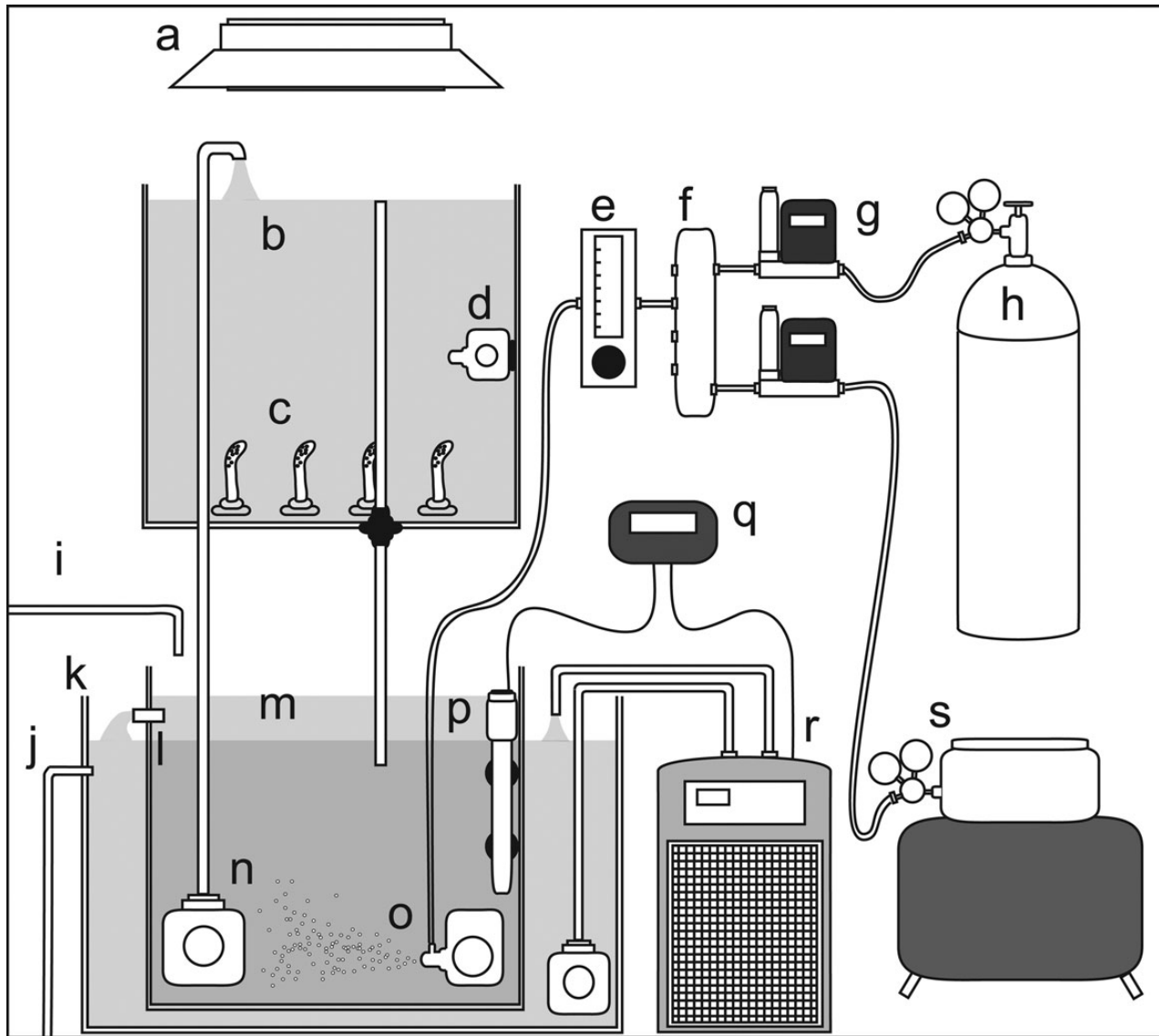


Figure 1. Experimental aquarium setup used to treat *E. flexuosa* with present-day and future carbonate chemistry conditions for 49 d. a, light; b, aquarium; c, octocorals; d, circulation pump; e, valved flowmeter; f, gas mixing chamber; g, mass flow controller; h, compressed CO₂ cylinder; i, fresh seawater input; j, seawater outflow; k, water bath; l, overflow; m, sump aquarium; n, water return pump; o, venturi pump; p, aquarium heater; q, microcontroller; r, chiller; s, air compressor.

Scanning procedure

Octocoral branch tips were scanned using a Skyscan 1174 micro-CT (Bruker) with a 50 kV, 800 μ A X-ray source. Samples were secured to the stage using parafilm and a 0.25 mm aluminium filter was used to block lower energy X-rays. Samples were scanned at a pixel resolution of 6.97 μ m using a 4400 ms exposure. X-ray images were collected every 0.7° over 180° of rotation. Flat images of X-ray transmittance, taken around the vertical axis, were reconstructed into a stack of transverse images using the NRecon software package (Figure 2). A 20% beam hardening correction factor, a ring artefact correction of four, and a dynamic range of 0.0–0.24 were consistently employed during reconstruction and were selected based on visual inspection and iterative optimization of multiple scans.

Analysis of micro-CT image stacks was conducted using CTAn. Regions of interest (ROI) were manually defined around the outer

surface of the first 2 mm of each apical branch tip. Growth rates of wild *E. flexuosa* reported from Puerto Rico range from 1.77 to 2.15 cm year⁻¹ (Yoshioka and Yoshioka, 1991), and the mean extension rates for individuals subjected to a transplant experiment were 1.55 cm year⁻¹ (Prada et al., 2008). The 2 mm used for analysis was therefore chosen as an estimate of new growth exclusively during experimental conditions (49 d). Calcification and sclerite formation likely also occurred outside of this apical region, though this area was excluded due to the difficulty of separating growth under experimental conditions from that which occurred prior. Volume, surface area, and mean attenuation coefficient of this region were recorded. Each of the 8-bit greyscale slices within the ROI was thresholded to create a binary image containing only high-density sclerites (Figure 2). The mean attenuation coefficient was recorded from this region and an ROI “shrink-wrapping”

function was applied to measure the volume and number of high-density sclerites. Per cent volume of sclerites was calculated by dividing the volume of the thresholded high-density regions by the total volume of the 2 mm branch tip.

Statistical analysis

Statistical analysis was performed using SPSS software (IBM, 2013). Variation in branch and sclerite parameters was investigated using general linear models (GLMs) with parent colony, $p\text{CO}_2$ treatment, and their interaction as factors. Upon finding the interaction effects non-significant ($p > 0.05$), they were removed and the analyses was re-run with main effects only.

Results

The mean temperature and salinity, as well as carbonate chemistry parameters (DIC, TA, calculated $p\text{CO}_2$, $x\text{CO}_2$), are shown for each tank and CO_2 treatment in Table 1. During the seventh week of the experiment, equipment malfunction resulted in an absence of DIC data, and consequently, calculated $p\text{CO}_2$ values are not

available for this week. However, tank and treatment averages for both TA and $x\text{CO}_2$ include data during this period. During week 4, TA was measured to be anomalously low in tanks 1–6 (2332.1 ± 1.0 , mean \pm s.e.m.), resulting in elevated calculated $p\text{CO}_2$.

Micro-CT was successful at resolving both octocoral branch morphology and internal high-density sclerites (Figure 3). Large middle cortex sclerites and smaller outer cortex sclerites were clearly visible in the reconstructed micro-CT scans, and were subsequently detected using thresholding of the higher-density materials (Figure 2a). No significant differences due to CO_2 treatments were detected among any of the branch (Figure 4, Tables 2 and 3) or sclerite (Figure 5, Tables 3 and 4) metrics. Significant parent colony effects were detected for branch extension and sclerite volume (Table 3).

Discussion

The absence of significant effects in *E. flexuosa* branch and sclerite morphology from CO_2 conditions projected to occur near the end

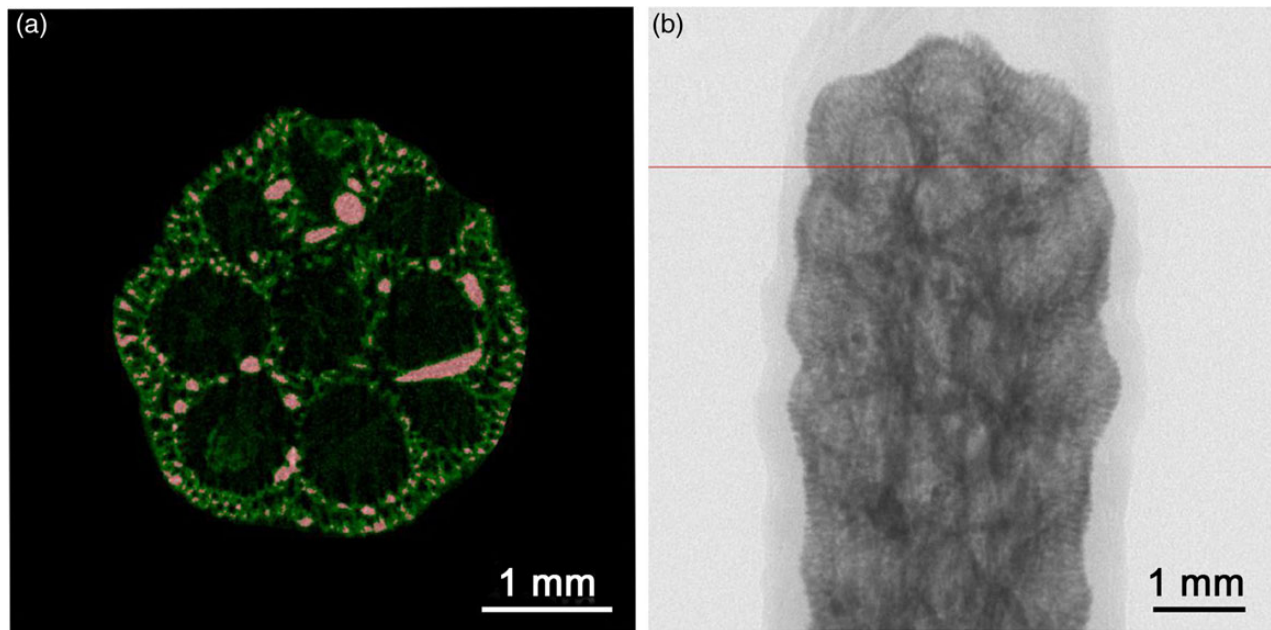


Figure 2. Two-dimensional micro-CT images of *E. flexuosa*. (a) Transverse section showing high-density sclerites thresholded in red and lower density structures in green; (b) coronal view X-ray transmittance. Red line in (b) denotes location of section in (a).

Table 1. Mean seawater parameters for each experimental tank as well as overall treatment means.

Tank	Temp. (°C)	Salinity (psu)	$x\text{CO}_2$ (ppm)	TA ($\mu\text{mol kg}^{-1}$)	DIC ($\mu\text{mol kg}^{-1}$)	pH (Total)	$p\text{CO}_2$ (μatm)	$\Omega_{\text{Aragonite}}$
Tank 1	24.8 (0.04)	36.6 (0.11)	446.5 (8.8)	2516.5 (27.36)	2216.7 (19.74)	7.99 (0.031)	516.5 (50.28)	3.45 (0.187)
Tank 2	24.7 (0.09)	36.5 (0.1)	443.8 (9.46)	2513.4 (26)	2204.3 (18.23)	8.01 (0.031)	493.1 (49.35)	3.55 (0.188)
Tank 3	24.3 (0.17)	36.5 (0.1)	429.4 (8.53)	2518 (26.49)	2213 (19.12)	8.01 (0.035)	493.1 (55.83)	3.5 (0.205)
Tank 4	24.5 (0.18)	36.5 (0.09)	437.1 (7.57)	2519.9 (27.93)	2211.9 (18.46)	8.01 (0.034)	487.9 (50.35)	3.54 (0.202)
Tank 5	24.8 (0.07)	36.6 (0.06)	1013.4 (64.99)	2516.7 (25.7)	2361 (28.7)	7.71 (0.063)	1196.1 (206.87)	2.09 (0.235)
Tank 6	24.6 (0.1)	36.6 (0.07)	998.1 (78.29)	2515.5 (25.29)	2344.2 (28.75)	7.75 (0.062)	1094.2 (229.3)	2.23 (0.223)
Tank 7	24.4 (0.21)	36.5 (0.08)	859.2 (53.01)	2520.4 (27.91)	2332.9 (28.18)	7.79 (0.055)	953 (165.85)	2.37 (0.222)
Tank 8	24.8 (0.13)	36.6 (0.08)	873 (47.27)	2537.1 (34.02)	2363.7 (33.5)	7.75 (0.059)	1079.3 (181.67)	2.25 (0.23)
L- CO_2	24.6 (0.07)	36.5 (0.05)	439.2 (4.29)	2517 (12.95)	2211.5 (9.11)	8.01 (0.016)	497.7 (24.81)	3.51 (0.094)
H- CO_2	24.6 (0.07)	36.5 (0.04)	934.9 (31.37)	2522.4 (13.73)	2350.5 (14.48)	7.75 (0.029)	1080.6 (95.84)	2.23 (0.111)

Parameter periodicity as reported in the Methods section. $x\text{CO}_2$ values measured with an infrared gas analyser and equilibrator. pH, $p\text{CO}_2$, Ω calculated from TA and DIC. Standard error in parentheses.

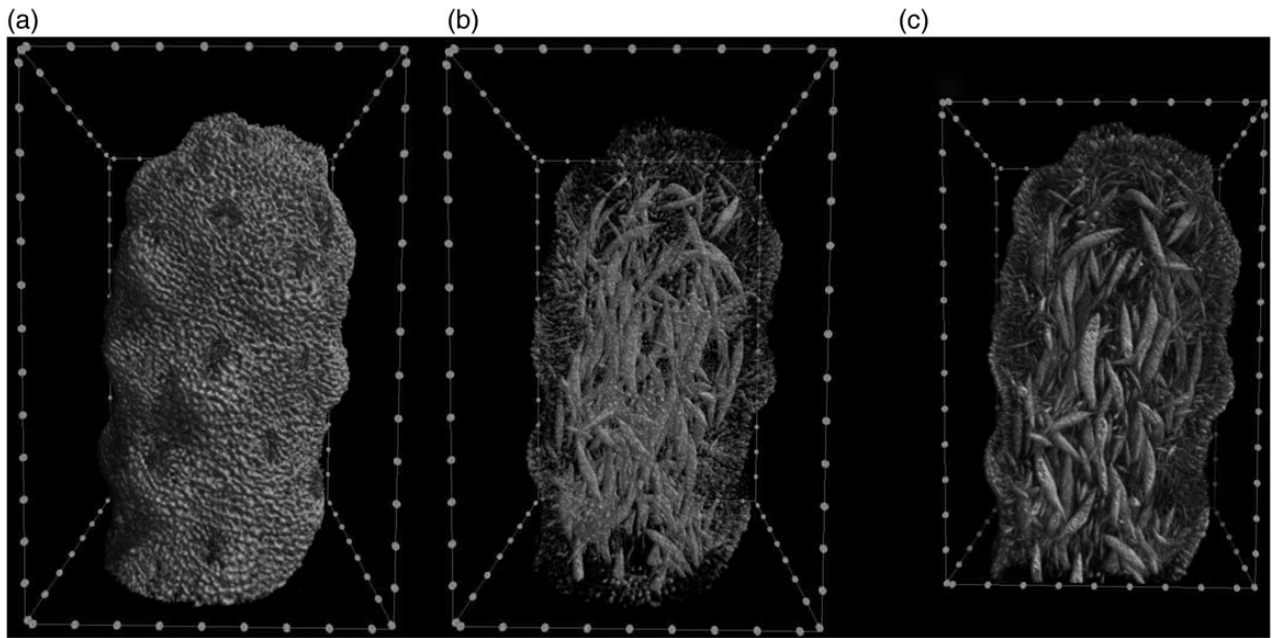


Figure 3. Micro-CT scans of *E. flexuosa*. (a) Surface of branch tip; (b) increased transparency showing high-density sclerites within branch tip; (c) digitally sectioned scan showing internal structure of branch tip. Spheres along margins of bounding boxes are 500 μm apart.

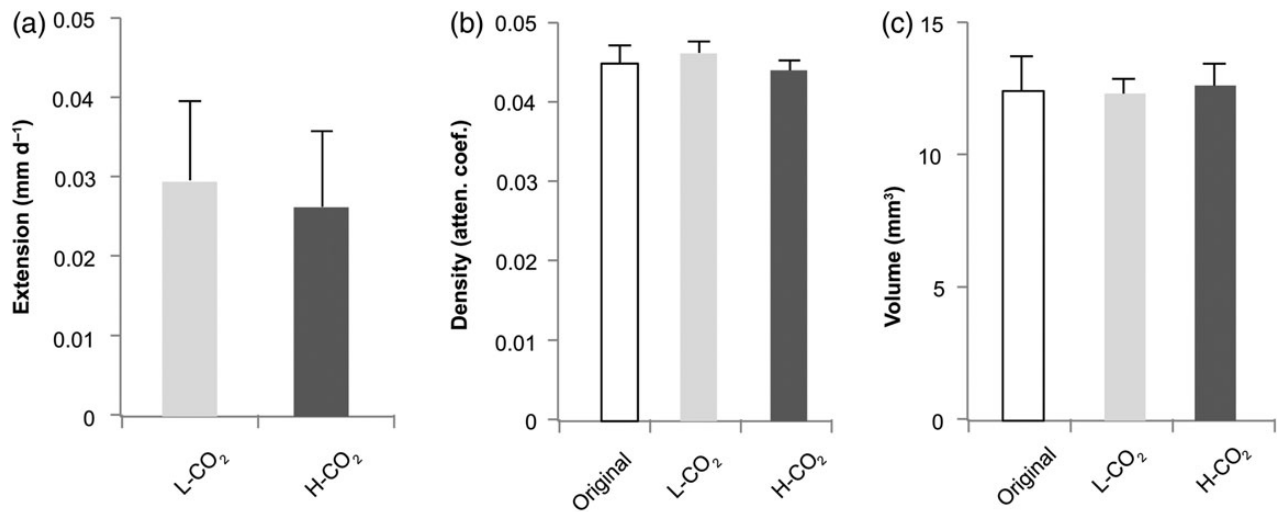


Figure 4. The response of *E. flexuosa* branches to low (L-CO₂, $n = 14$) and high CO₂ (H-CO₂, $n = 15$) conditions, as well as original branch characteristics. (a) Linear extension; (b) density of top 2 mm of branch tip; (c) volume of top 2 mm of branch tip. Error bars are standard error. No significant differences detected among L-CO₂ and H-CO₂ treatment means.

of the century are consistent with the findings of Gabay *et al.* (2013), who found no significant differences in the response of three species of octocorals, subjected to $p\text{CO}_2$ treatments more extreme (up to 3898 μatm) than those tested here (1081 μatm). While linear extension, branch morphology, and sclerite morphology were not directly measured in that study, they found no significant differences in protein and chlorophyll concentration, polyp and sclerite weight, zooxanthellae density, or polyp pulsation rate. Similarly and also consistent with our study, Gabay *et al.* (2014) used s.e.m. to visualize sclerite morphology and found no significant evidence of

degradation within living colonies of *Ovabunda manrospiculata*. In apparent contrast to the work of Gabay *et al.* (2014), Gómez *et al.* (2014) found significant negative correlation between $p\text{CO}_2$ and weight, linear extension, and the uptake of calcein stain into sclerites of *E. fusca*. *Eunicea fusca* is a congeneric of the *E. flexuosa*, used in this study, and while a significant relationship between $p\text{CO}_2$ and growth was observed in their study, extreme $p\text{CO}_2$ treatments (4568 μatm) were much greater than treatments utilized herein. Similar to our findings, however, when samples were subjected to CO₂ values predicted by the end of the century, differences

Table 2. Treatment and colony averages for *E. flexuosa* branch characteristics.

	Branch dens. (atten. coef.)	Branch vol. (mm ³)	Branch SA (mm ²)	Branch extension (mm d ⁻¹)
L-CO ₂	0.046 (0.0013)	12.31 (0.498)	35.33 (0.987)	0.03 (0.01)
Colony 1	0.049 (0.0022)	12.70 (0.509)	34.91 (0.895)	0.03 (0.014)
Colony 2	0.041 (0.0020)	11.88 (0.254)	34.87 (1.21)	0.00 (0.013)
Colony 3	0.047 (0.0023)	11.34 (0.808)	34.26 (1.316)	0.06 (0.027)
Colony 4	0.046 (0.0034)	13.51 (2.021)	37.79 (4.357)	0.02 (0.013)
H-CO ₂	0.044 (0.0011)	12.61 (0.725)	36.46 (1.543)	0.03 (0.010)
Colony 1	0.047 (0.0009)	14.36 (2.466)	39.59 (5.048)	0.02 (0.013)
Colony 2	0.042 (0.0010)	10.99 (1.479)	33.97 (3.708)	0.02 (0.017)
Colony 3	0.044 (0.0033)	11.27 (0.883)	33.97 (2.295)	0.06 (0.025)
Colony 4	0.044 (0.0022)	14.27 (0.178)	39.1 (1.013)	0.00 (0.000)
Total	0.045 (0.0009)	12.47 (0.438)	35.92 (0.920)	0.03 (0.007)
Initial	0.045 (0.0021)	12.41 (1.379)	35.18 (2.762)	n.a.

Initial values calculated as the mean of each parent colony sampled in advance of the experiment. Standard error in parentheses.

Table 3. Results of GLM analysis of branch and sclerite characteristics.

	Dependent variable	Source	d.f.	MS	F	p-value
Branch characteristics	Density	CO ₂	1	1.95E-05	1.078	0.309
		Colony	3	5.19E-05	2.864	0.058
		Error	24	1.81E-05	-	-
	Volume	CO ₂	1	0.858	0.18	0.675
		Colony	3	13.615	2.853	0.058
		Error	24	4.771	-	-
	Surface area	CO ₂	1	9.366	0.388	0.539
		Colony	3	32.718	1.356	0.28
		Error	24	24.137	-	-
	Extension	CO ₂	1	5.47E-06	0.005	0.944
		Colony	3	0.004	3.714	0.025
		Error	24	0.001	-	-
Sclerite characteristics	Density	CO ₂	1	2.77E-08	1.707	0.204
		Colony	3	7.55E-09	0.465	0.71
		Error	24	1.62E-08	-	-
	Volume	CO ₂	1	0.1	0.32	0.577
		Colony	3	1.394	4.446	0.013
		Error	24	0.314	-	-
	Surface area	CO ₂	1	543.521	0.281	0.601
		Colony	3	4207.539	2.178	0.117
		Error	24	1931.403	-	-
	Per cent volume	CO ₂	1	19.205	1.61	0.217
		Colony	3	29.552	2.477	0.086
		Error	24	11.93	-	-
	Count	CO ₂	1	1 310 904	0.021	0.887
		Colony	3	237 055 402.7	3.763	0.024
		Error	24	62 997 773.5	-	-

Note that all initial models included Colony × CO₂ treatment interaction terms; however, as these all emerged as non-significant, only main effects model results are shown.

Table 4. Treatment and colony averages for *E. flexuosa* sclerites characteristics.

	Sclerite dens. (atten. coef.)	Sclerite vol. (mm ³)	Sclerite SA (mm ²)	Per cent sclerite vol.	Count
L-CO ₂	0.24 (0.0000)	2.69 (0.154)	232.92 (9.93)	21.9 (1.09)	20 344.6 (1879.94)
Colony 1	0.24 (0.0000)	3.07 (0.184)	248.3 (14.971)	24.3 (1.71)	21 540.8 (2550.90)
Colony 2	0.24 (0.0000)	2.10 (0.176)	204.38 (13.573)	17.8 (1.87)	14 383.3 (1546.91)
Colony 3	0.24 (0.0001)	2.61 (0.396)	231.94 (28.516)	22.7 (1.86)	19 350.5 (5235.76)
Colony 4	0.24 (0.0002)	2.85 (0.140)	242.28 (11.091)	21.9 (2.68)	26 036.7 (1178.43)
H-CO ₂	0.24 (0.0000)	2.50 (0.188)	220.31 (13.978)	19.9 (0.87)	20 483.3 (2742.86)
Colony 1	0.24 (0.0000)	3.26 (0.640)	270.36 (55.734)	22.5 (0.54)	27 778.0 (11587.82)
Colony 2	0.24 (0.0000)	2.08 (0.287)	190.99 (26.536)	18.9 (0.88)	13 853.5 (2894.35)
Colony 3	0.24 (0.0000)	2.24 (0.208)	212.83 (8.881)	20.3 (2.46)	15 387.5 (1276.07)
Colony 4	0.24 (0.0000)	2.64 (0.232)	219.55 (12.296)	18.6 (1.88)	26 737.8 (2205.40)
Total	0.24 (0.0000)	2.59 (0.121)	226.4 (8.605)	20.9 (0.71)	20 416.3 (1654.69)
Initial	0.24 (0.0000)	2.57 (0.315)	206.86 (27.247)	20.79 (1.45)	22 318.3 (5737.50)

Initial values calculated as the mean of each parent colony sampled in advance of the experiment. Standard error in parentheses.

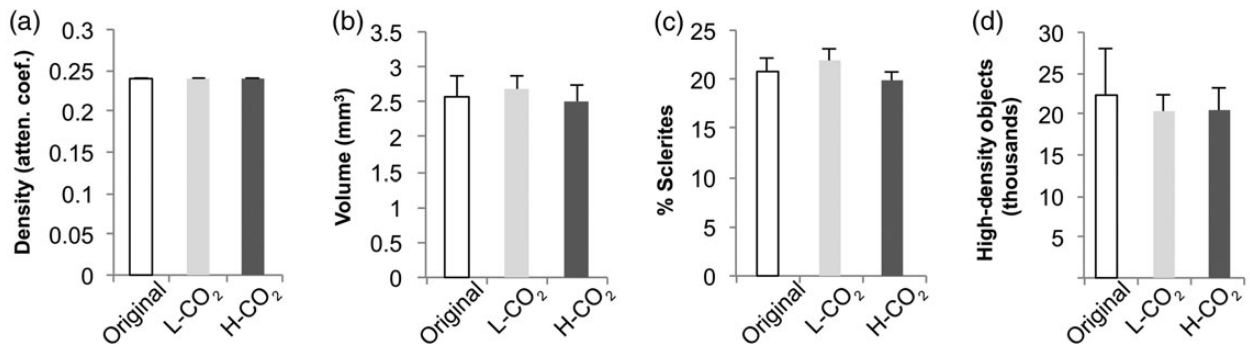


Figure 5. The response of sclerites in the top 2 mm tip of *E. flexuosa* branches to low (L-CO₂) and high CO₂ (H-CO₂) conditions, as well as original sclerites characteristics at the time of collection. (a) Total sclerite volume; (b) density of sclerites; (c) per cent volume of sclerites in the upper 2 mm of the branch tip; (d) number of high-density sclerites in upper 2 mm of branch tip as determined by thresholding micro-CT scans. Error bars are standard error. No significant differences detected among L-CO₂ and H-CO₂ treatment means.

in growth and calcification were not as apparent. In their study, as pCO₂ increased from 285 to 709 μatm, calcification was actually observed to increase.

Field-based evidence of the resilience of octocorals to OA and corroboration of the findings reported herein can be found in Inoue *et al.* (2013). Naturally occurring high CO₂ vents at Iwotorishima, Japan, mimic OA conditions projected for the end of the century. While nearby and unaffected ecosystems are dominated by scleractinian corals, those experiencing 831 μatm pCO₂ are dominated by *S. elegans*, and those experiencing 524 μatm pCO₂ have high densities of *Simularia* spp. The presence of these soft coral species in elevated CO₂, presumably for durations greatly more than experimental studies, underscores the resilience of these taxa to OA stress. It is worth noting, however, that in closer proximity to the vent where CO₂ conditions reached 1465 μatm, few octocorals were found. It is therefore possible that this reflects a threshold that limits the distribution of these taxa, although this is in apparent contrast to shorter experimental studies.

We cannot completely eliminate the potential that OA does indeed significantly affect *E. flexuosa*, yet we were unable to detect the subtle differences utilizing our methodologies. Given our novel high-precision technique and our analysis of actively calcifying branch tips, coupled with the agreement of our results with similar species in the literature, we find this unlikely. This is especially true under realistic OA scenarios and considering levels of response that are physiologically and ecologically relevant. We do not dispute, therefore, that under extreme levels of OA outside that predicted for the next 100 years, octocoral growth and calcification may be influenced by CO₂ (Gómez *et al.*, 2014).

Among the more-sensitive scleractinian hexacorals, considerable evidence has pointed to differential susceptibility of various species and genera to OA stress (Fabricius *et al.*, 2011; McCulloch *et al.*, 2012; Takahashi and Kurihara, 2012). Persistence of the calcification process despite reduced pH may be related to tissue separating the site of calcification from low pH water (Rodolfo-Metalpa *et al.*, 2011). For example, Gabay *et al.* (2014) observed that sclerites removed from living octocoral tissue experienced degradation and dissolution at extremely low pH's, while those within protective layers of live tissue were unaffected.

Shirur *et al.* (2014) have measured especially high calcified sclerite mass relative to organic tissues within *E. flexuosa* (81% dry tissue), indicating a high degree of calcification occurs within this species. Octocoral calcification is complicated, poorly understood,

and very different from that of hexacorals. Sclerite formation is initiated in the vacuole of scleroblasts contained in the mesoglea (Kingsley and Watabe, 1982). This vacuole contains a proteinaceous organic matrix or framework on which the sclerites are formed, and has been shown to be closely involved in regulating the structure and calcification of these sclerites (Rahman *et al.*, 2007; Rahman and Oomori, 2008). The vacuole increases in size as the sclerite calcifies, until the vacuole and cell membrane fuse and the sclerite transitions into the intercellular space (Kingsley and Watabe, 1982). This intracellular sclerite calcification is fundamentally different from the extracellular and extra-organismal skeletogenesis of scleractinian hexacorals (Cohen and McConnaughey, 2003). Indeed, this difference may be responsible for the relative stability of octocoral calcification, despite altered carbonate chemistry.

In addition to sclerite structures found within the mesoglea, holaxonian gorgonians have an axial skeleton made of gorgonin, a collagen and protein matrix that surrounds hollow canals. Internal cavities or loculi within this skeleton often contain calcified material, especially within the base and branches of colonies (Bond *et al.*, 2005). In some species (e.g. *Plexaurella dichotoma*), the spherulitic crystalline structure of these deposits indicates rapid formation via biological means (Bond *et al.*, 2005). However, in *E. flexuosa*, crystal shapes indicative of non-biogenic calcium carbonate precipitation have been observed (Lewis *et al.*, 1992), suggesting an internal environment highly conducive to calcification. X-ray diffraction of these crystals conducted by Lewis *et al.* (1992) revealed an unidentified diffraction pattern and an indeterminate crystal structure, though Lowenstam (1964) had previously sampled aragonite from within *E. flexuosa*. It remains to be seen if these structures respond differently to OA conditions than sclerites, though evidence indicates that they exist in a controlled internal environment, favourable for calcification.

Octocorals have highly diverse colony morphologies, both internally and externally. Colony shapes can be whip-like, fan-like, arborescent, or laminar and can vary with respect to their density and tissue thickness. Internally, they have many shapes and types of sclerites that differ in their distance from colony surfaces (Lewis and Von Wallis, 1991). These differences should be considered when evaluating the influence of OA on additional octocoral species and, as pointed out by Gabay *et al.* (2014), likely explain the apparent incongruities among previously published literature. For example, significant effects of OA have been measured in the relatively thin-tissued genus

Corallium, but not in the more fleshy genus *Sarcophyton* (Bramanti *et al.*, 2013; Gabay *et al.*, 2013).

While previous studies have referenced the high-magnesian calcite structure of sclerites (>4 mol%), we caution that this does not necessarily translate into high solubility and greater OA susceptibility. The relationship between magnesium content and solubility is poorly understood and somewhat contentious (Morse and Mackenzie, 1990). Concentrations of MgCO₃ vary greatly among octocoral species, but range from roughly 6 to 11 mol% (Velimirov and Böhm, 1976; Weinbauer and Velimirov, 1995). While older studies calculate higher solubility (e.g. Plummer and Mackenzie, 1974), in Morse and Mackenzie's (1990, Table 3.7) biogenic "best fit" curve, mole percentages of MgCO₃ <10 are not that different from aragonite with respect to solubility. In contrast, present-day MgCO₃ mole percentages for crustose coralline algae may be 18% (Ries, 2006), translating to a much higher solubility (Morse and Mackenzie, 1990), and resulting in a strong sensitivity to OA (Kuffner *et al.*, 2007). The only reported decline in calcification reported for an octocoral under conditions predicted for the end of the century has been for *C. rubrum* (Bramanti *et al.*, 2013). Microprobe investigation of the Mg content of their skeletons reveals values lower than what can be considered high-magnesian calcite, though subsequent X-ray analysis reveals much higher concentrations of 11.6 mol% (reviewed in Long *et al.*, 2014). Further research is needed to examine the relationship between magnesium concentration and solubility, especially with respect to the molecular composition of octocoral sclerites and their ability to withstand OA.

In addition to OA stress, coral reefs are impacted by climate change through increased SSTs, potentially leading to coral bleaching and mortality (Hoegh-Guldberg *et al.*, 2007). While octocorals are also known to bleach due to thermal stress, the long-term impact on their survivability may not be as severe as for hermatypic corals. In fact, relative to hexacorals, there are few documented cases in the scientific literature of Caribbean octocorals bleaching (Lasker *et al.*, 1984; Harvell *et al.*, 2001; Prada *et al.*, 2009). Prada *et al.* (2009) documented a high temperature event in Puerto Rico in 2005, resulting in 18% of octocorals bleaching, including colonies of *E. flexuosa*. Although individuals in the genus *Muricea* suffered mortality as a result of the event, most species and colonies recovered, and the overall mortality was low. While bleaching may occur cryptically in some octocoral species (with little change in colour), extreme 1983 ENSO-related warming resulted in no appreciable change in zooxanthellae densities in the octocoral *Plexaura kuna*, despite extensive bleaching and mortality of nearby scleractinian corals (Lasker, 2003).

The resistance to bleaching and OA stress demonstrated by several species of octocorals potentially indicates a degree of resilience to global change, especially with respect to structure, rigidity, and growth, of which sclerites play an important role (Lewis and Von Wallis, 1991). In the absence of other stressors (e.g. sedimentation, eutrophication, and overfishing), these data suggest that octocorals may become increasingly more prominent members of Caribbean reef ecosystems. Indeed, while scleractinian corals have steadily declined throughout the Caribbean (Gardner *et al.*, 2003), octocoral populations in the Florida Keys have generally increased since the mid-1990s, especially in shallow forereef habitats (Ruzicka *et al.*, 2013). Similarly, in St John, US Virgin Islands, octocoral abundances have remained relatively stable, while scleractinian coral populations have experienced dramatic declines (Colvard and Edmunds, 2011; Edmunds, 2013). While octocorals do provide habitat to associated invertebrates and fish, they lack

the permanence and structural complexity of scleractinian corals. Consequently, a shift from hermatypic scleractinians to octocorals may nevertheless correspond to a loss in reef ecosystem function.

Acknowledgements

We gratefully acknowledge funding from NOAA's CRCP and OAP.

References

- Albright, R., Mason, B., Miller, M., and Langdon, C. 2010. Ocean acidification compromises recruitment success of the threatened Caribbean coral *Acropora palmata*. *Proceedings of the National Academy of Sciences of the United States of America*, 107: 20400–20404.
- Alcolado, P. M., Claro-Madruga, R., Menéndez-Macias, G., García-Parrado, P., Martínez-Daranas, B., and Sosa, M. 2003. The Cuban coral reefs. In *Latin American Coral Reefs*, pp. 53–75. Ed. by J. Cortés. Elsevier, Amsterdam. 497 pp.
- Alvarez-Filip, L., Dulvy, N. K., Gill, J. A., Cote, I. M., and Watkinson, A. R. 2009. Flattening of Caribbean coral reefs: region-wide declines in architectural complexity. *Proceedings of the Royal Society B*, 276: 3019–3025.
- Baker, A. C., Glynn, P. W., and Riegl, B. 2008. Climate change and coral reef bleaching: an ecological assessment of long-term impacts, recovery trends and future outlook. *Estuarine, Coastal and Shelf Science*, 80: 435–471.
- Bignami, S., Enochs, I. C., Manzello, D. P., Sponaugle, S., and Cowen, R. K. 2013. Ocean acidification alters the otoliths of a pantropical fish species with implications for sensory function. *Proceedings of the National Academy of Sciences of the United States of America*, 110: 7366–7370.
- Bond, Z. A., Cohen, A. L., Smith, S. R., and Jenkins, W. J. 2005. Growth and composition of high-Mg calcite in the skeleton of a Bermudian gorgonian (*Plexaurella dichotoma*): potential for paleothermometry. *Geochemistry, Geophysics, Geosystems*, 6: 1–10.
- Bramanti, L., Movilla, J., Guron, M., Calvo, E., Gori, A., Dominguez-Carrió, C., Grinyó, J., *et al.* 2013. Detrimental effects of ocean acidification on the economically important Mediterranean red coral (*Corallium rubrum*). *Global Change Biology*, 19: 1897–1908.
- Cohen, A. L., and McConnaughey, T. A. 2003. Geochemical perspectives on coral mineralization. *Reviews in Mineralogy and Geochemistry*, 54: 151–187.
- Collins, M., Knutti, R., Arblaster, J., Dufresne, J-L., Fichefet, T., Friedlingstein, P., Gao, X., *et al.* 2013. Long-term climate change: projections, commitments and irreversibility. In *Climate Change 2013: the Physical Science Basis. Contribution of Working Group I to the Fifth Assessment Report of the Intergovernmental Panel on Climate Change*. Ed. by T. F. Stocker, D. Qin, G-K. Plattner, M. Tignor, S. K. Allen, J. Boschung, A. Nauels, *et al.* Cambridge University Press, Cambridge, UK and New York, NY.
- Colvard, N. B., and Edmunds, P. J. 2011. Decadal-scale changes in abundance of non-scleractinian invertebrates on a Caribbean coral reef. *Journal of Experimental Marine Biology and Ecology*, 397: 153–160.
- Cryonak, T., Schulz, K. G., and Joliel, P. L. 2016. The Omega myth: what really drives lower calcification rates in an acidifying ocean. *ICES Journal of Marine Science*, 73: 558–562.
- Diaz-Pulido, G., Gouezo, M., Tilbrook, B., Dove, S., and Anthony, K. R. 2011. High CO₂ enhances the competitive strength of seaweeds over corals. *Ecology Letters*, 14: 156–162.
- Dickson, A. G. 1990. Thermodynamics of the dissociation of boric acid in synthetic seawater from 273.15 to 318.15 K. *Deep Sea Research*, 37: 755–766.
- Dickson, A. G., and Millero, F. J. 1987. A comparison of the equilibrium constants for the dissociation of carbonic acid in seawater media. *Deep Sea Research*, 34: 1733–1743.

- Edmunds, P. J. 2013. Decadal-scale changes in the community structure of coral reefs of St. John, US Virgin Islands. *Marine Ecology Progress Series*, 489: 107–123.
- Enochs, I. C., Manzello, D. P., Carlton, R. D., Graham, D. M., Ruzicka, R., and Colella, M. A. 2015. Ocean acidification enhances the bioerosion of a common coral reef sponge: implications for the persistence of the Florida Reef Tract. *Bulletin of Marine Science*, 91: 271–290.
- Fabricius, K. E., Langdon, C., Uthicke, S., Humphrey, C., Noonan, S., De'ath, G., Okazaki, R., et al. 2011. Losers and winners in coral reefs acclimatized to elevated carbon dioxide concentrations. *Nature Climate Change*, 1: 165–169.
- Gabay, Y., Benayahu, Y., and Fine, M. 2013. Does elevated pCO₂ affect reef octocorals? *Ecology and Evolution*, 3: 465–473.
- Gabay, Y., Fine, M., Barkay, Z., and Benayahu, Y. 2014. Octocoral tissue provides protection from declining oceanic pH. *PLoS One*, 9: e91553.
- Gardner, T. A., Cote, I. M., Gill, J. A., Grant, A., and Watkinson, A. R. 2003. Long-term region-wide declines in Caribbean corals. *Science*, 301: 958–960.
- Glynn, P. W., and Enoch, I. C. 2011. Invertebrates and their roles in coral reef ecosystems. *In Coral Reefs: an Ecosystem in Transition*, pp. 273–325. Ed. by Z. Dubinsky, and N. Stambler. Springer, New York. 552 pp.
- Goh, N. K. C., Ng, P. K. L., and Chou, L. M. 1999. Notes on the shallow water gorgonian-associated fauna on coral reefs in Singapore. *Bulletin of Marine Science*, 65: 259–282.
- Gómez, C. E., Paul, V. J., Ritson-Williams, R., Muehllehner, N., Langdon, C., and Sánchez, J. A. 2014. Responses of the tropical gorgonian coral *Eunicea fusca* to ocean acidification conditions. *Coral Reefs*, 34: 451–460.
- Graham, N. A. J., and Nash, K. L. 2013. The importance of structural complexity in coral reef ecosystems. *Coral Reefs*, 32: 315–326.
- Guzmán, H. M. 2003. Caribbean coral reefs of Panamá: present status and future perspectives. *In Latin American Coral Reefs*, pp. 241–274. Ed. by J. Cortés. Elsevier, Amsterdam. 497 pp.
- Harvell, D., Kim, K., Quirolo, C., Weir, J., and Smith, G. 2001. Coral bleaching and disease: contributors to 1998 mass mortality in *Briareum asbestinum* (Octocorallia, Gorgonacea). *Hydrobiologia*, 460: 97–104.
- Hoegh-Guldberg, O., Mumby, P. J., Hooten, A. J., Steneck, R. S., Greenfield, P., Gomez, E., Harvell, C. D., et al. 2007. Coral reefs under rapid climate change and ocean acidification. *Science*, 318: 1737–1742.
- IBM. 2013. IBM SPSS Statistics for Windows. Armonk, NY.
- Inoue, S., Kayanne, H., Yamamoto, S., and Kurihara, H. 2013. Spatial community shift from hard to soft corals in acidified water. *Nature Climate Change*, 3: 683–687.
- IPCC. 2007. Climate change 2007: the physical science basis. *In Contribution of Working Group I to the Fourth Assessment Report of the Intergovernmental Panel on Climate Change*. Ed. by S. Solomon, D. Qin, M. Manning, Z. Chen, M. Marquis, K. B. Averyt, M. Tignor, et al. Cambridge University Press, Cambridge, UK and New York, NY.
- Jeng, M. S., Huang, H. D., Dai, C. F., Hsiao, Y. C., and Benayahu, Y. 2011. Sclerite calcification and reef-building in the fleshy octocoral genus *Sinularia* (Octocorallia: Alcyonacea). *Coral Reefs*, 30: 925–933.
- Johnson, V. R., Russell, B. D., Fabricius, K. E., Brownlee, C., and Hall-Spencer, J. M. 2012. Temperate and tropical brown macroalgae thrive, despite decalcification, along natural CO₂ gradients. *Global Change Biology*, 18: 2792–2803.
- Jokiel, P. L. 2016. Predicting the impact of ocean acidification on coral reefs: evaluating the assumptions involved. *ICES Journal of Marine Science*, 73: 550–557.
- Kingsley, R. J., and Watabe, N. 1982. Ultrastructural investigation of spicule formation in the gorgonian *Leptogorgia virgulata* (Lamarck) (Coelenterata: Gorgonacea). *Cell and Tissue Research*, 223: 325–334.
- Kleypas, J. A., Buddemeier, R. W., Archer, D., Gattuso, J. P., Langdon, C., and Opdyke, B. N. 1999. Geochemical consequences of increased atmospheric carbon dioxide on coral reefs. *Science*, 284: 118–120.
- Kroeker, K. J., Kordas, R. L., Crim, R. N., and Singh, G. G. 2010. Meta-analysis reveals negative yet variable effects of ocean acidification on marine organisms. *Ecology Letters*, 13: 1419–1434.
- Kroeker, K. J., Micheli, F., and Gambi, M. C. 2012. Ocean acidification causes ecosystem shifts via altered competitive interactions. *Nature Climate Change*, 3: 156–159.
- Kuffner, I. B., Andersson, A. J., Jokiel, P. L., Rodgers, K. u. S., and Mackenzie, F. T. 2007. Decreased abundance of crustose coralline algae due to ocean acidification. *Nature Geoscience*, 1: 114–117.
- Langdon, C., and Atkinson, M. 2005. Effect of elevated pCO₂ on photosynthesis and calcification of corals and interactions with seasonal change in temperature/irradiance and nutrient enrichment. *Journal of Geophysical Research*, 110: C09S07.
- Lasker, H. R. 2003. Zooxanthella densities within a Caribbean octocoral during bleaching and non-bleaching years. *Coral Reefs*, 22: 23–26.
- Lasker, H. R., and Coffroth, M. A. 1983. Octocoral distributions at Carrie Bow Cay, Belize. *Marine Ecology Progress Series*, 13: 21–28.
- Lasker, H. R., Peters, E. C., and Coffroth, M. A. 1984. Bleaching of reef coelenterates in the San-Blas Islands, Panama. *Coral Reefs*, 3: 183–190.
- Lewis, E., and Wallace, D. 1998. Program Developed for CO₂ System Calculations. ORNL/CDIAC, Oak Ridge, TN.
- Lewis, J. C., and Von Wallis, E. 1991. The function of surface sclerites in gorgonians (Coelenterata, Octocorallia). *The Biological Bulletin*, 181: 275–288.
- Lewis, J. C., Barnowski, T. F., and Telesnicki, G. J. 1992. Characteristics of carbonates of gorgonian axes (Coelenterata, Octocorallia). *The Biological Bulletin*, 183: 278–296.
- Long, X., Ma, Y., and Qi, L. 2014. Biogenic and synthetic high magnesium calcite—a review. *Journal of Structural Biology*, 185: 1–14.
- Lowenstam, H. A. 1964. Coexisting calcites and aragonites from skeletal carbonates of marine organisms and their strontium and magnesium contents. *In Recent Researches in the Fields of Hydrosphere, Atmosphere and Nuclear Geochemistry*, pp. 373–404. Ed. by Y. Miyake, and T. Koyama. Maruzen Co., Ltd, Tokyo.
- McCulloch, M., Falter, J., Trotter, J., and Montagna, P. 2012. Coral resilience to ocean acidification and global warming through pH up-regulation. *Nature Climate Change*, 2: 623–627.
- Mehrbach, C., Culbertson, C. H., Hawley, J. E., and Pytkowicz, R. M. 1973. Measurement of the apparent dissociation constants of carbonic acid in seawater at atmospheric pressure. *Limnology and Oceanography*, 18: 897–907.
- Morales Pinzón, A., Orkisz, M., Rodríguez Useche, C. M., Torres González, J. S., Teillaud, S., Armando Sánchez, J., and Hernández Hoyos, M. 2014. A semi-automatic method to extract canal pathways in 3D micro-CT images of octocorals. *PLoS ONE*, 9: e85557.
- Morse, J. W., and Mackenzie, F. T. 1990. *Geochemistry of Sedimentary Carbonates*. Elsevier, New York. 707 pp.
- Plummer, L. N., and Mackenzie, F. T. 1974. Predicting mineral solubility from rate data: application to the dissolution of magnesian calcites. *American Journal of Science*, 274: 61–83.
- Prada, C., Schizas, N. V., and Yoshioka, P. M. 2008. Phenotypic plasticity or speciation? A case from a clonal marine organism. *BMC Evolutionary Biology*, 8: 47.
- Prada, C., Weil, E., and Yoshioka, P. M. 2009. Octocoral bleaching during unusual thermal stress. *Coral Reefs*, 29: 41–45.
- Rahman, M. A., and Oomori, T. 2008. Structure, crystallization and mineral composition of sclerites in the alcyonarian coral. *Journal of Crystal Growth*, 310: 3528–3534.
- Rahman, M. A., Oomori, T., and Uehara, T. 2007. Carbonic anhydrase in calcified endoskeleton: novel activity in biocalcification in alcyonarian. *Marine Biotechnology*, 10: 31–38.
- Reaka-Kudla, M. L. 1997. The global biodiversity of coral reefs: a comparison with rain forests. *In Biodiversity II*, pp. 83–108. Ed. by M. W.

- Reaka-Kudla, D. E. Wilson, and E. O. Wilson. Joseph Henry Press, Washington, DC.
- Rhein, M., Rintoul, S. R., Aoki, S., Campos, E., Chambers, D., Feely, R. A., Gulev, S., *et al.* 2013. Observation: Ocean. *In* Climate Change 2013: the Physical Science Basis. Contribution of Working Group I to the Fifth Assessment Report of the Intergovernmental Panel on Climate Change. Ed. by T. F. Stocker, D. Qin, G-K. Plattner, M. Tignor, S. K. Allen, J. Boschung, A. Nauels, *et al.* Cambridge University Press, Cambridge, UK and New York, NY.
- Ries, J. B. 2006. Mg fractionation in crustose coralline algae: geochemical, biological, and sedimentological implications of secular variation in the Mg/Ca ratio of seawater. *Geochimica et Cosmochimica Acta*, 70: 891–900.
- Rodolfo-Metalpa, R., Houlbrèque, F., Tambutté, É., Boisson, F., Baggini, C., Patti, F. P., Jeffree, R., *et al.* 2011. Coral and mollusc resistance to ocean acidification adversely affected by warming. *Nature Climate Change*, 1: 308–312.
- Ruzicka, R. R., Colella, M. A., Porter, J. W., Morrison, J. M., Kidney, J. A., Brinkhuis, V., Lunz, K. S., *et al.* 2013. Temporal changes in benthic assemblages on Florida Keys reefs 11 years after the 1997/1998 El Niño. *Marine Ecology Progress Series*, 489: 125–141.
- Shirur, K. P., Ramsby, B. D., Iglesias-Prieto, R. I., and Goulet, T. L. 2014. Biochemical composition of Caribbean gorgonians: implications for gorgonian—*Symbiodinium* symbiosis and ecology. *Journal of Experimental Marine Biology and Ecology*, 461: 275–285.
- Takahashi, A., and Kurihara, H. 2012. Ocean acidification does not affect the physiology of the tropical coral *Acropora digitifera* during a 5-week experiment. *Coral Reefs*, 32: 305–314.
- Velimirov, B., and Böhm, E. L. 1976. Calcium and magnesium carbonate concentrations in different growth regions of gorgonians. *Marine Biology*, 35: 269–275.
- Weinbauer, M. G., and Velimirov, B. 1995. Calcium, magnesium and strontium concentrations in the calcite sclerites of Mediterranean gorgonians (Coelenterata: Octocorallia). *Estuarine, Coastal and Shelf Science*, 40: 87–104.
- Yoshioka, P. M., and Yoshioka, B. B. 1989. Multispecies, multiscale analysis of spatial pattern and its application to a shallow-water gorgonian community. *Marine Ecology Progress Series*, 54: 257–264.
- Yoshioka, P. M., and Yoshioka, B. B. 1991. A comparison of the survivorship and growth of shallow-water gorgonian species of Puerto Rico. *Marine Ecology Progress Series*, 69: 253–260.

Handling editor: Joanna Norkko